Journal of Power Sources 240 (2013) 530–535

Contents lists available at SciVerse ScienceDirect

Journal of Power Sources

journal homepage: www.elsevier.com/locate/jpowsour

Effects of Na^+ contents on electrochemical properties of $Li_{1.2}Ni_{0.13}Co_{0.13}Mn_{0.54}O_2$ cathode materials

Bao Qiu, Jun Wang, Yonggao Xia*, Yuanzhuang Liu, Laifen Qin, Xiayin Yao, Zhaoping Liu*

Ningbo Institute of Material Technology & Engineering, Chinese Academy of Sciences, Ningbo 315201, PR China

HIGHLIGHTS

- A small amount of Na^+ can significantly increase the initial discharge capacity.
- Some of the Na^+ ions could be reversibly de-/re-intercalated from the electrodes.
- The structure evolves from a solely layered structure to a mixture of layered structure.
- It could explain how the sodium species impact on the electrochemical performance.

ARTICLE INFO

Article history:
Received 24 December 2012
Received in revised form
6 April 2013
Accepted 10 April 2013
Available online 23 April 2013

Keywords:
Cathode material
Sodium-ions content
Layered lithium-excess
Solid solution
Lithium-ion batteries

ABSTRACT

The $Li_{1.2-x}Na_xNi_{0.13}Co_{0.13}Mn_{0.54}O_2$ ($0 \le x \le 0.1$) cathode materials have been synthesized by a solid-state reaction method. The effects of the Na^+ contents on the structure, surface components and electrochemical performance are studied by X-ray diffraction (XRD), X-ray photoelectron spectroscopy (XPS) and electrochemical techniques. The XRD data indicate that the $Li_{1.2-x}Na_xNi_{0.13}Co_{0.13}Mn_{0.54}O_2$ samples evolve from a sole layered structure ($0 \le x \le 0.02$) to a mixture of Na^+-contained layered structure ($0.02 < x \le 0.1$), which would transform into the single layered structure after the initial charge and discharge process. XPS data demonstrate that some of the Na^+ ions could be reversibly de-/re-intercalated for the $Li_{1.2-x}Na_xNi_{0.13}Co_{0.13}Mn_{0.54}O_2$ materials. An electrochemical test reveals that a small amount of Na^+ ($x \le 0.02$) in the $Li_{1.2-x}Na_xNi_{0.13}Co_{0.13}Mn_{0.54}O_2$ materials can significantly increase the rate capacity, yet the capacity retention becomes worse. We also find that the capacity retention increases with the Na^+ contents.

1. Introduction

In order to fulfill the energy density of Li-ions batteries for the requirements of plug-in hybrid electric vehicles (PHEVs) or all-electric vehicles (EVs), lithium-excess layered transition-metal oxides, e.g. $Li_{1.2}Ni_{0.13}Co_{0.13}Mn_{0.54}O_2$ or $Li_{1.2}Ni_{0.2}Mn_{0.6}O_2$, have been widely investigated as very appealing cathode materials for the Lithium-ion batteries [1–4]. The most attractive advantage of these materials is their large discharge capacity of over 250 mAh g^{-1}, which supplies twice the energy density of the commercial $LiCoO_2$, $LiMn_2O_4$, and $LiFePO_4$ cathode materials. However, several disadvantages such as poor rate performance, cycling capability decay and a large initial irreversible capacity (IRC) loss, are the main obstacles for their practical application in lithium-ion battery systems [4].

Until now, many attempts have been made to overcome these drawbacks of the lithium-excess layered transition-metal oxides using various preparation techniques, such as molten salt [5,6], ion exchange [7,8], co-precipitation [9,10], and so on. For example, the composites $xLi_2MnO_3 \cdot (1-x)LiMn_{1/3}Ni_{1/3}Co_{1/3}O_2$ were prepared by a two-step molten-salt method using Na^+-contained compounds as the reaction medium which was thoroughly washed with distilled water. The prepared sample with $x = 0.3$ showed improved rate capability at elevated temperature, but the capacity retention was only 64% after 20 cycles [5]. Recently, Kim et al. [7] reported that the $Li_x(Ni_{0.25}Mn_{0.75})O_y$ samples could be synthesized by the ion-exchange reaction from layered Na^+-contained $Na_{0.9}Li_{0.3}Ni_{0.25}Mn_{0.75}O_\delta$ precursor. It showed extremely high-power performance, but relatively low discharge capacity. Even though the final mixture was washed out with distilled water or applied with Li^+/Na^+ ion-exchange reaction to exhaustively remove the Na^+ species, a certain amount of insoluble or adsorbed Na^+ species still resided in samples, which have been detected by ICP or XPS [5,7]. Moreover, it is well known that the co-precipitation method with soluble transition-metal salts using hydroxide or carbonate as precipitant is widely applied to the laboratory-scale and industrial syntheses of

* Corresponding authors. Tel./fax: +86 574 8668 5096.
E-mail addresses: xiayg@nimte.ac.cn (Y. Xia), liuzp@nimte.ac.cn (Z. Liu).

0378-7753/$ – see front matter
http://dx.doi.org/10.1016/j.jpowsour.2013.04.047

lithium-excess layered transition-metal oxides. However, the initial discharge capacity of one material with same composition always varied in a broad range even under the same measurement condition [11,12]. Since the precipitant of the co-precipitation process is usually sodium hydroxide or carbonate, and the existence of Na^+ cannot be avoided in the final sample, even after extensively rinsing. Therefore, lithium-excess layered transition-metal oxide materials synthesized by these methods contain the sodium species more or less in the final samples, which may directly influence their electrochemical performance.

To the best of our knowledge, the effect of the residual Na^+ on the electrochemical performance of the lithium-excess layered cathode materials has not been investigated so far, accompanying with the situations that Na^+ contents in the composites are still lack of the quantitative control. In addition, it is important to clarify the electrochemical mechanism about the Na^+ ions in the materials during the charge/discharge process. In this work, we synthesized the $Li_{1.2-x}Na_xNi_{0.13}Co_{0.13}Mn_{0.54}O_2$ ($0 \le x \le 0.1$) with Li^+ substituted by Na^+ using a solid-state reaction method, and discussed the effects of Na^+ contents on the structure and electrochemical performance in detail.

2. Experimental

2.1. Preparation

The $Li_{1.2-x}Na_xNi_{0.13}Co_{0.13}Mn_{0.54}O_2$ ($0 \le x \le 0.1$) samples were synthesized by a solid-state reaction method as reported previously [13]. The raw materials are lithium hydroxide [$LiOH \cdot H_2O$] (99.5%, Sinophar), sodium hydroxide [NaOH] (99%, Sinophar), nickel acetate [$Ni(CH_3COO)_2 \cdot 4H_2O$] (99.9%, Sinophar), manganese acetate [$Mn(CH_3COO)_2 \cdot 4H_2O$] (99.5%, Sinophar), cobalt acetate [$Co(CH_3COO)_2 \cdot 4H_2O$] (99.9%, Sinophar), and oxalic acid (99.9%, Sinophar). They were mixed stoichiometrically and calcined by two steps, which were firstly pre-treated at 500 °C for 5 h under air and then calcined at 850 °C for 20 h with a heating rate of 5 °C min^{-1}. Note that all the samples were synthesized under the same condition to ensure the comparability of the results.

2.2. Characterization

The as-prepared samples were characterized by X-ray powder diffraction (XRD), using an AXS D8 Advance diffractometer (reflection $\theta-\theta$ geometry, Cu-Ka radiation, receiving slit 0.2 mm, scintillation counter, 40 mA, 40 kV) from Bruker, Inc. The chemical compositions of the samples were confirmed quantitatively by inductive coupled plasma (ICP) with an emission spectrometer (Optima 2100 DV, Perkin–Elmer). X-ray photoelectron spectroscopy (XPS) measurements were conducted using an AXIS Ultra DLD spectrometer with Al-Kα (1253.6 eV) radiation. To collect the initial charge/discharge cathode active material powders, coin-type cells were disassembled in an argon-filled glove box, washed with anhydrous dimethyl carbonate (DMC), and dried under vacuum for overnight. The sample powders were scraped off and used for further XRD and XPS analyses to determine the changes of the structure and the Na^+ contents in the electrodes.

2.3. Electrochemical measurements

Electrochemical properties of the $Li_{1.2-x}Na_xNi_{0.13}Co_{0.13}Mn_{0.54}O_2$ ($0 \le x \le 0.1$) electrodes were measured after assembling them into coin cells (type CR2032) in an argon-filled glove box. The cathode was prepared by spreading a mixture of active material (80 wt.%), acetylene black (10 wt.%), and poly (vinylidene fluoride) binder (10 wt.%) dissolved in N-methyl pyrrolidone onto an aluminum foil current collector. The cathode was separated from the lithium anode by a separator (Celgard 2502). The density of the active material for electrode was around 6 mg cm^{-2}. The electrolyte (Zhangjiagang Guotai-Huarong New Chemical Materials Co., Ltd.) is 1 M $LiPF_6$, dissolved into a mixture of ethylene carbonate (EC)/DMC (3:7, v/v). The galvanostatical charge and discharge tests were carried out under a constant current density between 2.0 and 4.8 V on a battery tester (LAND-CT2001A, Jinnuo Wuhan Co., Ltd., P. R. China). The current density of 250 mA g^{-1} is equal to the 1 C rate.

Table 1
The experimental (exp.) and theoretical (th.) results of Na/Li and Li/(Ni + Co + Mn) ratios of the $Li_{1.2-x}Na_xNi_{0.13}Co_{0.13}Mn_{0.54}O_2$ samples.

Samples	Na/Li ($\times 10^{-3}$)		Li/(Ni + Co + Mn)	
	th.	exp.	th.	exp.
$x = 0$	0	0	1.500	1.440
$x = 0.005$	4.18	0	1.490	1.411
$x = 0.01$	8.40	1.80	1.487	1.424
$x = 0.02$	16.95	26.80	1.475	1.433
$x = 0.05$	43.48	48.64	1.438	1.405
$x = 0.1$	90.91	98.30	1.375	1.370

3. Results and discussion

The chemical composition of Li, Na, Ni, Co and Mn was measured by ICP, as shown in Table 1. It is demonstrated that the experimental Na/Li ($x/1-x$) and Li/(Mn + Ni + Co) ratios in the synthesized samples are close to the nominal values for the high Na^+ content samples ($x \ge 0.01$), indicating that little lithium was evaporated during the high temperature calcinations. However, for the composites with $x = 0.005$ and 0.01, the Na^+ content is too low to precisely detect, and so the experimental results are inconformity with the nominal values.

Fig. 1 shows the XRD patterns of the $Li_{1.2-x}Na_xNi_{0.13}Co_{0.13}Mn_{0.54}O_2$ ($0 \le x \le 0.1$) samples. The main reflections of all the samples could be indexed on the basis of a hexagonal *R-3m* unit cell, while the weak super-lattice reflections between 20° and 30° are ascribed to the Li_2MnO_3-like unit cell with monoclinic (*C2/m*) symmetry [14,15]. However, it is also found that a trace of impurity phase in the samples formed at high Na^+ contents ($x = 0.05$ and 0.1). The peak of impurity phase agrees with the result reported by Kim et al. [7,16], which can be well indexed to the hexagonal layered structure-type $Na_{0.7}MnO_{2+\alpha}$ ($0.05 \le \alpha < 1.3$). This result demonstrates that the increase of Na^+ content causes a transformation from a sole layered structure to a mixture of Na^+-contained

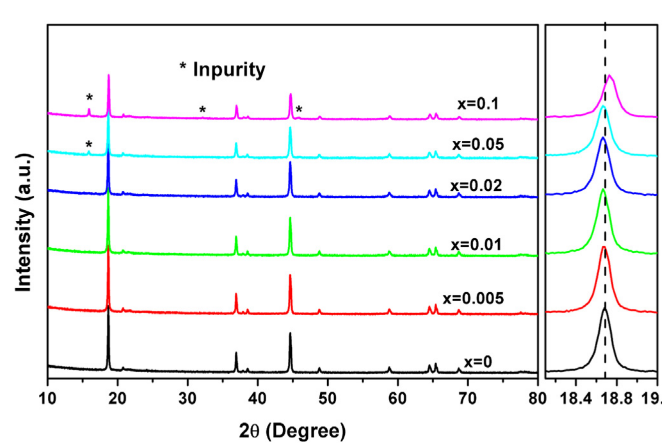

Fig. 1. XRD patterns of the $Li_{1.2-x}Na_xNi_{0.13}Co_{0.13}Mn_{0.54}O_2$ samples.

Table 2
Variations of lattice parameters *a*, *c* and *c*/*a* of the $Li_{1.2-x}Na_xNi_{0.13}Co_{0.13}Mn_{0.54}O_2$ samples with Na^+ content.

Samples	Pristine			Charge to 4.8 V			Discharge to 2.0 V		
	a (Å)	*c* (Å)	*c*/*a*	*a* (Å)	*c* (Å)	*c*/*a*	*a* (Å)	*c* (Å)	*c*/*a*
$x = 0$	2.8509	14.2274	4.9905	2.8382	14.2073	5.0057	2.8580	14.2815	4.9970
$x = 0.005$	2.8510	14.2306	4.9914	2.8352	14.2337	5.0204	2.8596	14.2928	4.9982
$x = 0.01$	2.8512	14.2370	4.9933	2.8368	14.3068	5.0387	2.8627	14.2946	4.9934
$x = 0.02$	2.8512	14.2369	4.9933	2.8394	14.3439	5.0517	2.8593	14.2937	4.9990
$x = 0.05$	2.8516	14.2366	4.9925	2.8332	14.2580	5.0325	2.8560	14.2655	4.9949
$x = 0.1$	2.8493	14.2014	4.9842	2.8402	14.3458	5.0510	2.8533	14.3205	5.1089

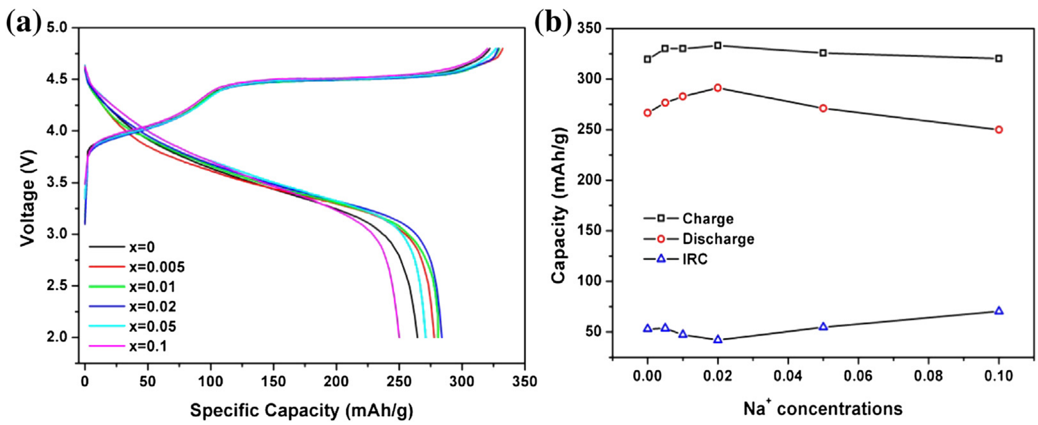

Fig. 2. (a) First charge–discharge curves and (b) the corresponding charge capacity, discharge capacity, IRC values of the $Li_{1.2-x}Na_xNi_{0.13}Co_{0.13}Mn_{0.54}O_2$ samples.

hexagonal layered structure. In addition, the enlargement of the XRD patterns in the 2θ range of 18°–19° is also displayed in Fig. 1, and indicates a shift to low angles from $x = 0$ to $x = 0.02$ due to the replacement of Li^+ by Na^+. And an inflection of shift to the high angles with the further increase of Na^+ content due to the formation of impurity sodium species.

Table 2 shows lattice parameters of the pristine $Li_{1.2-x}Na_xNi_{0.13}Co_{0.13}Mn_{0.54}O_2$ samples calculated by *Maud* Rietveld refinements from the X-ray diffraction data. The lattice parameters *a*, *c* and *c*/*a* increased with Na^+ content from $x = 0$ to $x = 0.02$, confirming the continuous substitutions of larger Na^+ for Li^+. And the lattice parameters decreased with $x = 0.05$ and 0.1 owing to the formation of impurity Na^+ species. As above mentioned, it is reasonable to believe that the excessive Na^+ leads to the formation of impure $Na_{0.7}MnO_{2+\alpha}$ phase when the Na^+ content reaches its limit in the host lattice.

Fig. 2(a) shows the first charge–discharge curves of the samples with various Na^+ contents at 0.1 C. All the samples exhibit a slope region (<4.5 V) attributed to the extraction of Li^+ ions from the lithium layer. In this process, the Ni^{2+} and Co^{3+} were oxidized to Ni^{4+} and $Co^{3.6+}$, respectively. Additionally, a long plateau region at ~4.5 V was observed for the whole samples, corresponding to the concomitant loss of oxygen from the lattice during the first charge as reported in the literature [14]. This process provides a high capacity in the subsequent cycling. The variations of the charge/discharge capacity and IRC with the increase of Na^+ content are summarized in the Fig. 2(b). It can be seen that the sample with the substitution of Na^+ as little as $x = 0.005$ for Li^+ increases the charge capacity sensitively from 319.4 to 330 mAh g^{-1}, as well as the discharge capacity from 266.5 to 276.5 mAh g^{-1}. Even when the sample with *x* increased to 0.02, the discharge capacity can reach 291 mAh g^{-1}, and the IRC is only about 42 mAh g^{-1}. It could be partly attributed to the increased *d*-spacing with the substitution of Li^+ by a small amount of Na^+ ions, as indicated by the XRD data (Fig. 1). Accordingly, it is confirmed that the charge/discharge capacity

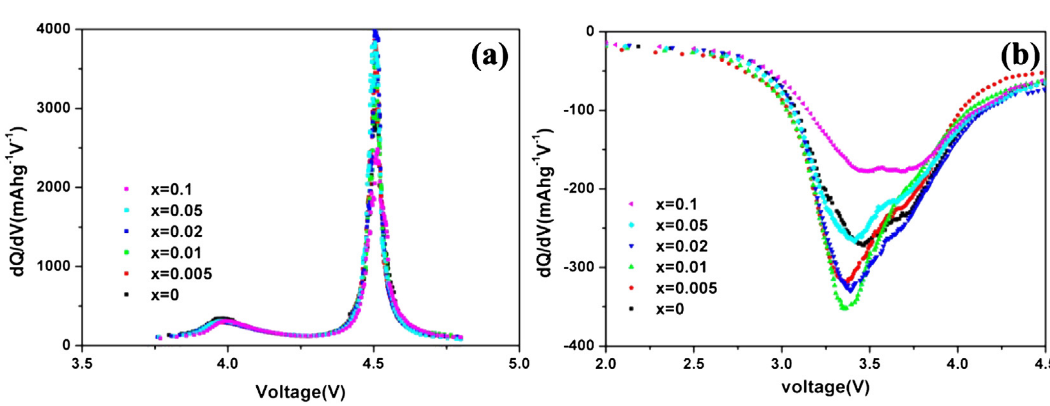

Fig. 3. Differential capacity (d*Q*/d*V*) plots of (a) the first charge, (b) the discharge curves of the $Li_{1.2-x}Na_xNi_{0.13}Co_{0.13}Mn_{0.54}O_2$ samples shown in Fig. 2(a).

and initial irreversible capacity loss of these samples can be significantly guided by the Na^+ content.

In order to specifically interpret the variations of the charge/discharge capacity with different Na^+ contents, dQ/dV (Q is specific capacity and V is the voltage of the cells) for checking the electrochemical redox reaction, are calculated from the numerical data observed in Fig. 2(a), and the dQ/dV *vs.* V plots are illustrated in Fig. 3. As shown in Fig. 3(a), there are two oxidation peaks in all the samples: a distinct broad oxidation peak at approximately 4.0 V and a sharp peak at around 4.5 V. The former could be assigned to the oxidation of nickel or cobalt ions and shifts to a higher voltage at a higher Na^+ content ($x = 0.05$ and 0.1) accompanied with the sodium species formation, which increases the degree of the electrode polarization. The latter is the electrochemical activation process of the Li_2MnO_3 component to form activated MnO_2 and has the strongest intensity at Na^+ content of $x = 0.02$, which indicates that the largest reversible capacity might be obtained after the discharge process. The dQ/dV plots of the discharge curves with all the cells are compared in Fig. 3(b). It is noted that the intensity of the peak at ~3.5 V, generally considered to be the reduction process of tetravalent manganese ions to trivalent manganese ions [17,18], significantly increases with the Na^+ content from $x = 0$ to $x = 0.02$, which indicates that much more activated MnO_2 exists in electrode material after the initial charge process and provides more vacancies for Li^+ insertion with high discharge capacity during the discharge process [17]. This result may origin from the enlarged interlayer resulting in the more Li^+ ions extracted from the electrode. However, with the Na^+ content increasing to $x = 0.1$, the intensity of the peak at ~3.5 V decreased due to the existence of less activated MnO_2 during the initial charge and larger polarization. In addition, the sample with $x = 0.02$ has the initial highest discharge capacity and the peak at ~3.5 V progressively shifts to a higher voltage. These results demonstrated that the Na^+ could significantly affect the activation degree of Li_2MnO_3 component possibly by itself extraction; however, the mechanism during the charge–discharge process is still unknown. As discussed above, after the Li_2MnO_3 component is activated, generated MnO_2 exists in the electrode material, which can insert Na^+ ions as well [16]. So it is speculated that it could be reinserted into the electrode, if the Na^+ can be extracted from the electrode during the charge process.

To determine the intercalation/de-intercalation behaviors of Na^+ ions in all the samples, XPS was carried out to investigate the variations of the surface Na^+-ions contents. Fig. 4(a) shows the Na 1s spectra recorded from the pristine electrodes for the $Li_{1.2-x}Na_xNi_{0.13}Co_{0.13}Mn_{0.54}O_2$ samples with different Na^+ contents. It can be observed that there is an increase in the relative intensity of the samples with Na^+ content. After the XPS tests, the pristine electrodes were charged to 4.8 V. Then the Na 1s peak recorded from the charged electrode is shown in Fig. 4(b). It is interesting that the Na^+ ions do not exist in the surface for all the electrodes. Thus, nearly 100% of the Na^+ ions were extracted from the electrode during the charge process, which is consistent with our speculation. The Na 1s peak recorded from the discharged electrode is also described in Fig. 4(c). Some Na^+ species were observed in the discharged electrode. The results are equally consistent with our analysis that the partly extracted Na^+ from the electrode could reinsert into the electrode.

From the above investigations, the Li-ions intercalated into the electrode, along with a certain number of Na-ions reinserted into the electrode during the first discharge. The consequence is that some Li-vacated active sites during the charge process may be occupied by Na-ions and become unavailable for Li^+ in the following discharge process, which directly influence the capacity retention. Fig. 5 presents the cycling behaviors of $Li_{1.2-x}Na_xNi_{0.13}Co_{0.13}Mn_{0.54}O_2$ samples at 0.5 C in the voltage range of 2.5–4.7 V. The smaller voltage range is benefit for getting a better cycle performance than that of 2–4.8 V as reported by Wei et al. [19]. As shown in the Fig. 5, the cycling performance was significantly dominated by the small amount of Na^+, even an increase in the discharge capacity was found for the samples with $x = 0.005$ and 0.01. The Na^+-free sample delivered a discharge capacity of 193.5 mAh g^{-1} with of the capacity retention of 96.5% after 50 cycles. Although the sample with $x = 0.005$ shows the highest initial discharge capacity of 221 mAh g^{-1}, the capacity retention was only 71.6% after 50 cycles. For the samples with $x = 0.01$, 0.02, 0.05, 0.1,

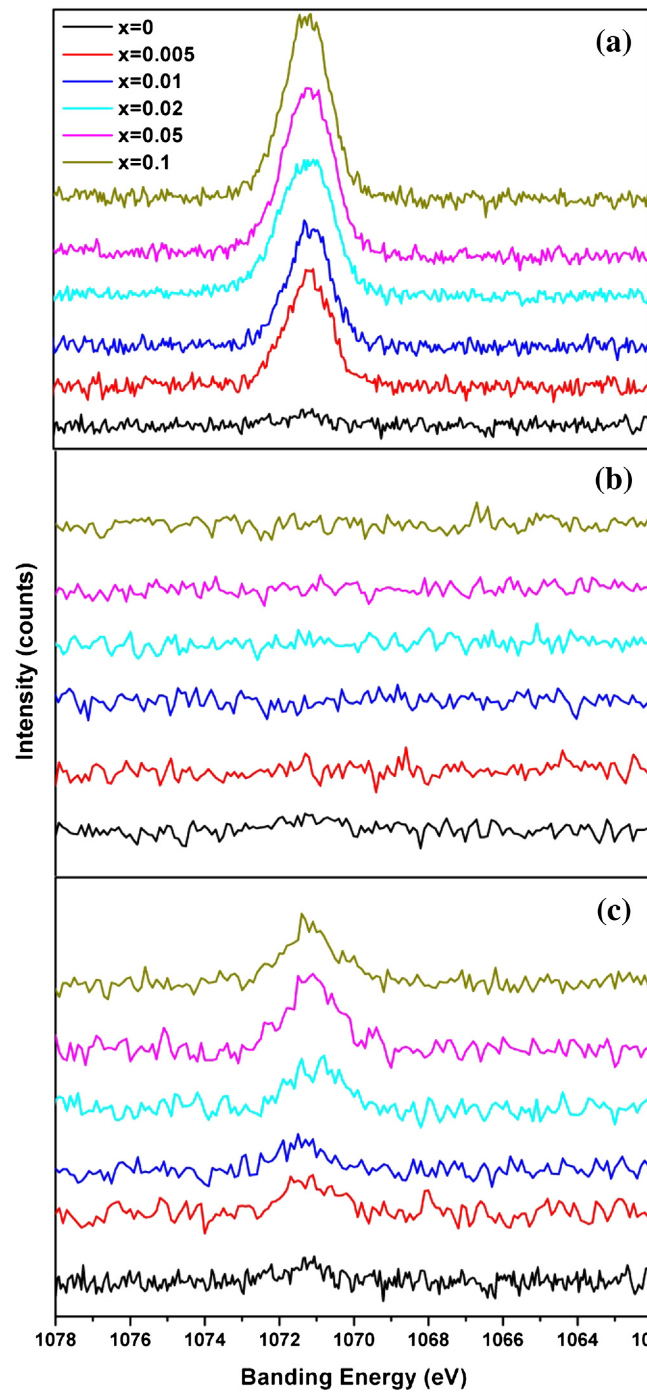

Fig. 4. XPS spectra of Na 2p of the $Li_{1.2-x}Na_xNi_{0.13}Co_{0.13}Mn_{0.54}O_2$ samples: (a) pristine material, (b) first charge to 4.8 V and (c) discharge to 2.0 V after the charge to 4.8 V at 0.1 C.

the capacity retentions were 74.1%, 77.8%, 79.9% and 92.1% after 50 cycles, respectively. Obviously, the capacity retention of these samples increases with the Na^+ content ($0.005 \le x \le 0.1$). The improved cycling performance is possibly ascribed to the structure stabilized with Na^+ ions by pillaring effects, which agrees with the results reported by Whittingham's group [20].

Fig. 6(a) shows the XRD patterns of the $Li_{1.2-x}Na_xNi_{0.13}Co_{0.13}Mn_{0.54}O_2$ electrodes after being initially charged to 4.8 V at 0.1 C. The intensity ratio of (003)/(104) for the Na^+-free sample decreases after the initial charge process, and the characteristic peaks of Li_2MnO_3 component disappear, which is contributed to the complete Li^+ extraction at the high potentials, resulting in the loss of the layeredness in the material [21,22]. However, the intensity ratio of (003)/(104) for the samples containing Na^+ ions has no big changes. This phenomenon indicates that the existence of Na^+ ions in the lithium-excess layered material can enhance the stability of the structure at the high potentials. An enlargement of the XRD patterns show that the (003) reflection shifts to lower 2θ angle when the Na^+ contents ranges from $x = 0$ to 0.02 as shown in Fig. 6(a). However, for the samples with $x = 0.05$ and 0.1, it is found that the impurity Na^+ species has disappeared from the XRD patterns after the first charge, and this indicates that the structural arrangement has occurred when the Na^+ ions were extracted from the electrode, which is consistent with the result in Na^+-ions batteries [23]. Consequently, the peak shift of (003) is possibly associated with the phase transition as a result of Na^+ extraction. This explanation is only served as a hypothesis, however, further related analysis of the structural changes in these hybrid components deserves investigations. The XRD patterns of the samples after being initially discharged to 2 V at 0.1 C are shown in Fig. 6(b). The XRD patterns of the samples from $x = 0$ to 0.02 are well agreed with that of the charged electrodes, associated with changes in the lattice parameters as a result of Li^+ intercalation. Table 2 shows the variations of the lattice parameters of the initial charge/discharge electrodes with Na^+ content. The variation trends of lattice parameters with the discharged electrode are consistent with the charged electrode for the samples with $x = 0.05$ and 0.1. From the *Ex situ* XRD diffraction data, they confirmed again that the Na^+ ions in the samples with $x = 0.005$, 0.01 and 0.02 only occupy in the interlayer, and can adjust the activation extent of the Li_2MnO_3 component to improve the electrochemical performance, while the samples with $x = 0.05$ and 0.1 form the impurity species, inducing the phase transition to increase the electrode polarization after electrochemical activation.

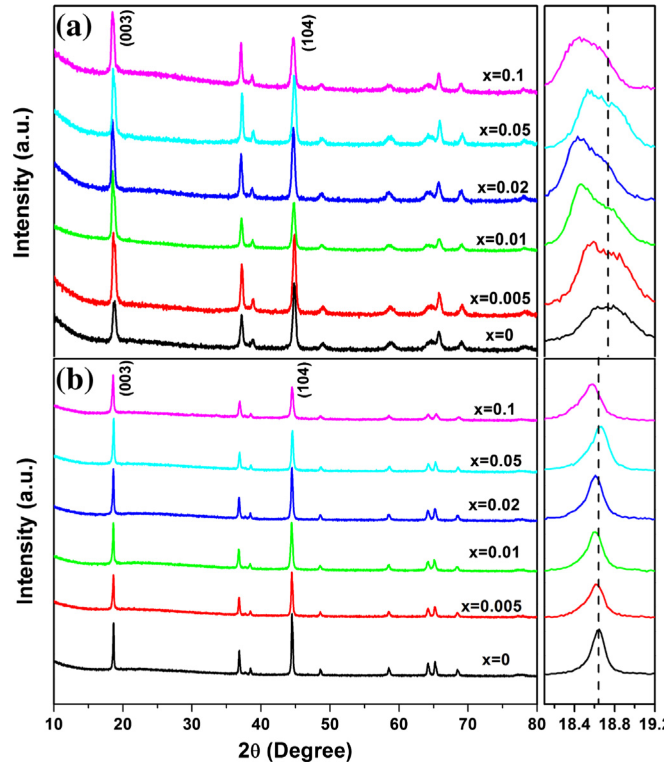

Fig. 6. *Ex situ* XRD patterns of the $Li_{1.2-x}Na_xNi_{0.13}Co_{0.13}Mn_{0.54}O_2$ samples: (a) initial charge to 4.8 V and (b) initial discharge to 2.0 V after initial charge to 4.8 V at 0.1 C.

To further investigate the effects of the Na^+ content on the rate capability, the discharge capacity of as-prepared cells were charged at 0.1 C rate and discharged at various C rates in the voltage range of 2.0–4.8 V, which was summarized in Fig. 7. It was found that the addition of a small amount of Na^+ ions ($0.05 \le x \le 0.02$) can significantly improve the rate capacity of $Li_{1.2-x}Na_xNi_{0.13}Co_{0.13}Mn_{0.54}O_2$ at all C rates. For instance, among these samples, the sample with $x = 0.02$ has the highest discharge capacity of 288 mAh g^{-1},

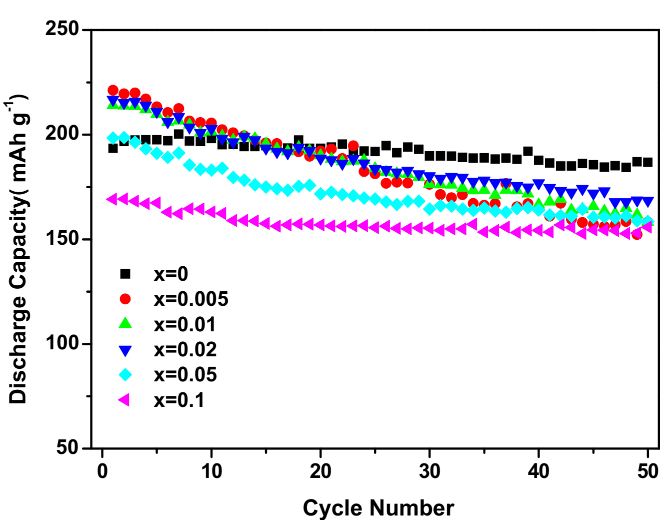

Fig. 5. Comparative cycling behaviors of $Li_{1.2-x}Na_xNi_{0.13}Co_{0.13}Mn_{0.54}O_2$ samples at 0.5 C between 2.5 V and 4.7 V.

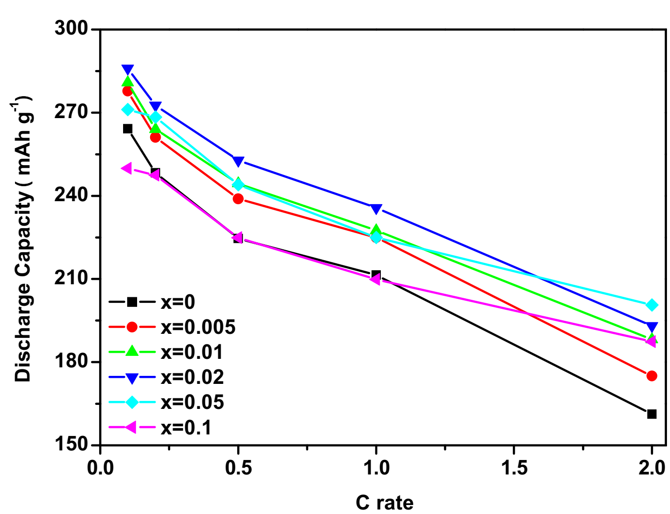

Fig. 7. Discharge capacity of $Li_{1.2-x}Na_xNi_{0.13}Co_{0.13}Mn_{0.54}O_2$ samples at different C rate in the voltage range of 2.0–4.8 V. The cells were charged at 0.1 C before discharge testing.

272 mAh g^{-1}, 252 mAh g^{-1}, 236 mAh g^{-1} and 193 mAh g^{-1} at 0.1 C, 0.2 C, 0.5 C, 1 C and 2 C, respectively. Perhaps it is the improved rate capacity that is related with its enlarged interlayer and pure layered structure. With the further increase of the Na^+ content ($x = 0.05$ and 0.1), the rate capacity of sample becomes worse, which may be ascribed to the presence of impurity phase. From above results, it is believed that the addition of Na^+ has greatly affected the rate capacity of $Li_{1.2-x}Na_xNi_{0.13}Co_{0.13}Mn_{0.54}O_2$ cathodes.

4. Conclusions

The Na^+ content in the lithium-excess layered cathode is an important factor, which affects its electrochemical performance. The addition of a small amount of Na^+ ions ($x \leq 0.02$) could significantly improve the rate capacity of $Li_{1.2-x}Na_xNi_{0.13}Co_{0.13}Mn_{0.54}O_2$, yet the cycling performance became deteriorated. It should be noted that the capacity retentions of Na additive samples increased with the Na^+ content. The improved cycling performance could be ascribed to the structure stabilized with Na^+ ions by pillaring effects. In addition, almost all the Na^+ ions in the electrode could be extracted from the electrode, but some of Na^+ ions could reinsert into the electrode. This work can explain how the composite with the sodium species in the Li-excess layered oxides impact on the electrochemical performance.

Acknowledgements

We are grateful for financial support from the Key Research Program of Chinese Academy of Sciences (Grant No. KGZD-EW-202-4), the 973 program (Grant No. 2011CB935900), the Natural Science Foundation of Ningbo (Grant No. 2012A610126) and Ningbo Science and Technology Innovation Team (Grant No. 2012B82001).

References

[1] M.M. Thackeray, C. Wolvertonb, E.D. Isaacsc, Energy. Environ. Sci. 5 (2012) 7854–7863.
[2] P. He, H.J. Yu, D. Li, H.S. Zhou, J. Mater. Chem. 22 (2012) 3680–3695.
[3] B.L. Ellis, K.T. Lee, L.F. Nazar, Chem. Mater. 22 (2010) 691–714.
[4] M.M. Thackeray, S.-H. Kang, C.S. Johnson, J.T. Vaughey, R. Benedeka, S.A. Hackney, J. Mater. Chem. 17 (2007) 3112–3125.
[5] C. Yu, G.S. Li, X.F. Guan, J. Zheng, L.P. Li, T.W. Chen, Electrochim. Acta 81 (2012) 283–291.
[6] J.L. Liu, L. Chen, M.Y. Hou, F. Wang, R.C. Che, Y.Y. Xia, J. Mater. Chem. 22 (2012) 25380–25387.
[7] D.H. Kim, S.-H. Kang, M. Balasubramanian, C.S. Johnson, Electrochem. Commun. 12 (2010) 1618–1621.
[8] S.-H. Kang, C.S. Johnson, J.T. Vaughey, K. Amine, M.M. Thackeray, J. Electrochem. Soc. 153 (2006) A1186–A1192.
[9] H.X. Deng, I. Belharouak, Y.-K. Sun, K. Amine, J. Mater. Chem. 19 (2009) 4510–4516.
[10] D.-K. Lee, S.-H. Park, K. Amine, H.J. Bang, J. Parakash, Y.-K. Sun, J. Power Sources 162 (2006) 1346–1350.
[11] J.-H. Lim, H. Bang, K.-S. Lee, K. Amine, Y.-K. Sun, J. Power Sources 189 (2009) 571–575.
[12] G. Singh, R. Thomas, A. Kumar, R.S. Katiyar, A. Manivannan, J. Electrochem. Soc. 159 (2012) A470–A478.
[13] J. Wang, B. Qiu, Y.G. Xia, Z.P. Liu, J. Power Sources 218 (2012) 128–133.
[14] R. Armstrong, M. Holzapfel, P. Novak, C.S. Johnson, S.H. Kang, M.M. Thackeray, P.G. Bruce, J. Am. Chem. Soc. 128 (2006) 8694–8698.
[15] Z.H. Lu, J.R. Danh, J. Electronchem. Soc. 149 (2002) A815–A822.
[16] D.H. Kim, S.-H. Kang, M. Slater, S. Road, J.T. Vaughey, N. Karan, M. Balasubramanian, C.S. Johnson, Adv. Energy. Mater. 1 (2011) 333–336.
[17] H.J. Yu, H. Kim, Y.R. Wang, P. He, D. Asakura, Y. Nakamura, H.S. Zhou, Phys. Chem. Chem. Phys. 14 (2012) 6548–6595.
[18] H.J. Yu, H.S. Zhou, J. Mater. Chem. 22 (2012) 15507–15510.
[19] Z. Li, F. Du, X.F. Bie, D. Zhang, Y.M. Cai, X.R. Cui, C.Z. Wang, G. Chen, Y.J. Wei, J. Phys. Chem. C 114 (2010) 22751–22757.
[20] P.K. Sharma, G.J. Moore, F. Zhang, P. Zavalij, M.S. Whittingham, Electrochem. Solid-State Lett. 2 (1999) 494–496.
[21] C.R. Fell, K.J. Carroll, M.F. Chi, Y.S. Meng, J. Electrochem. Soc. 157 (2010) A1202–A1211.
[22] F. Amalraj, D. Kovacheva, M. Talianker, L. Zeiri, J. Grinbat, N. Leifer, G. Goobes, B. Markovsky, D. Aurbach, J. Electrochem. Soc. 157 (2010) A1121–A1130.
[23] Z.H. Lu, J.R. Dahn, J. Electrochem. Soc. 148 (2001) A1225–A1229.